Spine Deformity

www.spine-deformity.org

Spine Deformity 4 (2016) 253–260

Biomechanics

Biomechanical Assessment of Providence Nighttime Brace for the Treatment of Adolescent Idiopathic Scoliosis

Amjad Sattout, MD, MASc[a,b], Julien Clin, PhD[a,b], Nikita Cobetto, MASc[a,b], Hubert Labelle, MD[b], Carl-Eric Aubin, PhD, PEng[a,b,*]

[a]*Department of Mechanical Engineering, Polytechnique Montréal, P.O. Box 6079, Downtown Station, Montreal, Quebec H3C 3A7, Canada*
[b]*Research Center, Sainte-Justine University Hospital Center, 3175 Côte-Sainte-Catherine Road, Montreal, Quebec H3T 1C5, Canada*

Received 27 March 2015; revised 22 December 2015; accepted 24 December 2015

Abstract

Study Design: Biomechanical study of the Providence brace for the treatment of adolescent idiopathic scoliosis (AIS).
Objectives: To model and assess the effectiveness of Providence nighttime brace.
Summary of Background Data: Providence nighttime brace is an alternative to traditional daytime thoracolumbosacral orthosis for the treatment of moderate scoliotic deformities. It applies three-point pressure to reduce scoliotic curves. The biomechanics of the supine position and Providence brace is still poorly understood.
Methods: Eighteen patients with AIS were recruited at our institution. For each patient, a personalized finite element model (FEM) of the trunk was created. The spine, rib cage, and pelvis geometry was acquired using simultaneous biplanar low-dose radiographs (EOS). The trunk surface was acquired using a three-dimensional surface topography scanner. The interior surface of each patient's Providence brace was digitized and used to generate an FEM of the brace. Pressures at the brace/skin interface were measured using pressure sensors, and the average pressure distribution was computed. The standing to supine transition and brace installation were computationally simulated.
Results: Simulated standing to supine position induced an average curve correction of 45% and 48% for thoracic and lumbar curves, while adding the brace resulted in an average correction of 62% and 64% (vs. real in-brace correction of 65% and 70%). Simulated pressures had the same distribution as measured ones. Bending moments on apical vertebrae were mostly annulled by the positioning in the supine position, and further overcorrected on average by 10% to 13%, but in the opposite direction.
Conclusions: The supine position is responsible for the major part of coronal curve correction, while the brace itself plays a complementary role. Bending moments induced by the brace generated a rebalancing of pressure on the growth plates, which could help reduce the asymmetric growth of the vertebrae.
Level of Evidence: Level II.

Keywords: Scoliosis; Nighttime brace; Providence brace; Finite element modeling; Biomechanics

Author disclosures: AS (grants from Natural Sciences and Engineering Research Council of Canada, from Canadian Institutes of Health Research, during the conduct of the study), JC (grants from Canadian Institutes of Health Research, grants from Natural Sciences and Engineering Research Council of Canada, during the conduct of the study; other from Rodin 4D, outside the submitted work), NC (grants from Natural Sciences and Research Council of Canada, grants from Canadian Institutes of Health Research, during the conduct of the study; other from Lagarrigue [Rodin4D], outside the submitted work), HL (grants from Natural Sciences and Research Council of Canada, grants from Canadian Institutes of Health Research, during the conduct of the study; other from Spinologics, grants from Depuy Synthes, outside the submitted work), C-EA (grants from Natural Sciences and Research Council of Canada, grants from Canadian Institutes of Health Research, during the conduct of the study; other from Groupe Lagarrigue, other from Boston Brace, grants and other from Natural Sciences and Engineering Research Council of Canada; Research Chair program with Medtronic of Canada, outside the submitted work).

Ethical approval: All procedures performed in this study involving human participants were in accordance with the ethical standards of the institutional ethical research committee. Informed consent was obtained from all individual participants included in the study and their parents.

*Corresponding author. Canada Research Chair in Orthopedic Engineering, Department of Mechanical Engineering, Polytechnique Montreal, P.O. Box 6079, Downtown Station, Montreal, Quebec H3C 3A7, Canada. Tel.: 1 (514) 340-4711x2836; fax: 1 (514) 340-5867.

E-mail address: carl-eric.aubin@polymtl.ca (C.-E. Aubin).

2212-134X/$ - see front matter © 2016 Scoliosis Research Society.
http://dx.doi.org/10.1016/j.jspd.2015.12.004

Introduction

Adolescent idiopathic scoliosis (AIS) is a complex three-dimensional (3D) deformity of the spine and rib cage. For small and moderate curves (Cobb angle 20 to 45°) with apex below the eighth thoracic vertebra (T8), conservative treatment by thoraco-lumbo-sacral orthoses (TLSOs) is the most common treatment to halt the curve progression until the end of skeletal growth. Bracing significantly decreases the progression of high-risk curves to surgery proportionally with longer hours of brace wear [1], and the risk for curve progression and surgery are reduced in patients with good brace compliance [2,3]. In order to effectively stop scoliotic curve progression, a day-time brace has to be worn more than 12 hours per day [1,4]. Compliance with full-time brace wearing is problematic. Patients wear their braces on average 46% of the time they were instructed to [4]. To overcome this longstanding problem, nighttime braces were developed. Nighttime bracing has less negative effect on psychosocial functioning, sleep disturbance, back pain, body image, and back flexibility [5]. In cases where different braces are equally effective, the recommended treatment would be the brace with the least impact on the quality of life [5].

There are different existing nighttime braces. Among them, the Charleston nighttime brace, introduced in 1978 by Price et al. relies on the principle of side bending to overcorrect the major scoliotic curve [6], and reduced brace wear to a minimum of 8 hours per night during sleep. Providence nighttime brace, introduced by d'Amato et al. in 1992, is based on direct lateral and rotational forces applied at the apex of curves through a three-point pressure system [7]. A CAD/CAM model is made based on the readings of the measurement board [8]. Published clinical studies reported an average initial in-brace correction of 94% for thoracic curves, 111% for thoracolumbar curves, 103% for lumbar curves, and 90% and 91% for double curves, respectively [7,9-11]. Often, overcorrection is observed on supine in-brace radiographs [7]. Overall success rate (curve progression $\leqslant 5°$ after minimum follow-up of 2 years beyond the cessation of brace wear) is 50% to 75% [7,11]. The recumbent position is also known to reduce the scoliotic curves, in particular during instrumentation surgeries [12,13].

Finite element models (FEMs) were developed to study brace biomechanics and improve the design of braces [14-17]. TLSOs are now simulated with a realistic representation of the contact interface between the patient's trunk and brace [18-20]. Using such approach, it was possible to quantify Charleston brace's biomechanical effects, such as the inversion of asymmetrical compressive loading in the major scoliotic curve, and the worsening of compressive loading in the compensatory curves [21]. The finite element modeling of daytime braces was also extensively done to assess the biomechanics of braces [17-22] and improve their design [20,23], as well as to study the effect of recumbent positioning [24]. In a recent ongoing randomized clinical trial, preliminary results of 40 patients showed that a novel design scheme combining CAD/CAM and 3D FEM simulation allowed the fabrication of more efficient and lighter braces compared to the use of CAD/CAM only [25].

Although Providence brace has been available for more than 20 years, the biomechanics of this treatment as well as the specific effects of brace design parameters and of the recumbent position are still not well described. The CAD/CAM model is chosen from a brace data bank based on mold inventory [8], then subjected to derotation of the thoracic section. The impact of brace design and adjustments on outcomes are not well understood, as no evaluation method is used before brace fabrication. The objective of this study was therefore to biomechanically model and assess the Providence nighttime brace for the treatment of AIS in order to better understand its mode of action.

Materials and Methods

Patient data

Inclusion criteria were diagnosis of AIS by the treating orthopedic surgeon, age 10–16 years at time of Providence brace prescription, thoracic and/or lumbar curve Cobb angle 20–45 degrees, and first time or renewal brace. Exclusion criteria were non-idiopathic scoliosis and previous spine surgery.

Patient and brace FEMs

For each case, the internal osseous anatomy (spine, rib cage, and pelvis) was reconstructed in 3D using a simultaneous biplanar low-dose system (EOS imaging SA, Paris, France) [26,27]. The accuracy of this technique is 1.0 mm for the spine and pelvis and 1.9 mm for the rib cage [26,27]. A free-form interpolation technique was used to generate a detailed 3D model of the spine, pelvis, and rib cage based on anatomic reference points. The external geometry (skin surface) of the trunk was acquired using a 3D surface topography technique (3-dimensional Capturor; Creaform Inc., Lévis, Canada) [28]. Internal and external geometries were registered by applying a point-to-point least square algorithm to 12 radiopaque markers attached to anatomic landmarks on the patient's torso [29].

A personalized FEM of each patient's trunk was then created using ANSYS 14.5 software package (ANSYS Inc., Canonsburg, PA, USA) by methods previously validated [21]. This model includes the thoracic and lumbar vertebrae, intervertebral discs, ribs, sternum, costal cartilages, abdominal cavity, and pelvis, which were represented by 3D elastic beam elements. The zygapophyseal joints were modeled by shells and contact elements, the vertebral and intercostal ligaments by tension-only spring elements, and

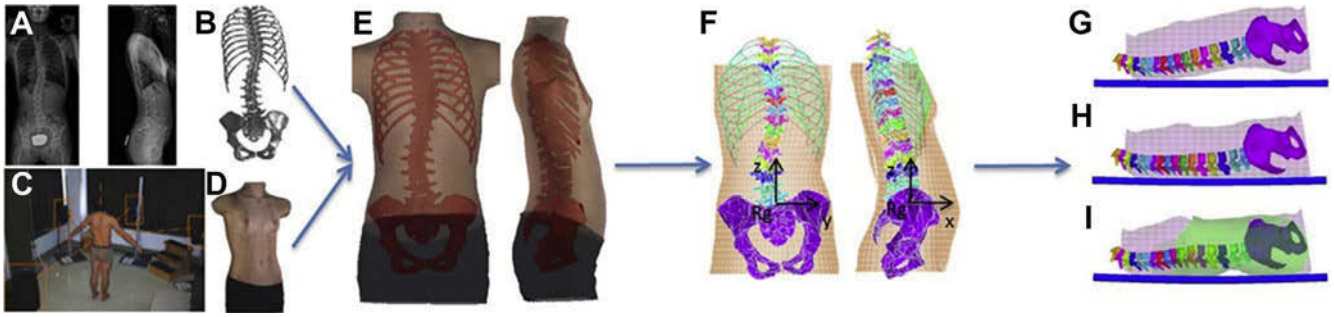

Fig. 1. Building patient's finite element model. (A) Acquisition of the osseous geometry using biplanar radiographs. (B) 3D Reconstruction of the internal osseous geometry. (C) Acquisition of patient's external geometry using surface topography. (D) 3D reconstruction of external surface geometry. (E) Combining internal and external geometries. (F) Finite element model (Rg: Global coordinate system) (ligaments not shown for clarity. (G) Initial supine configuration (without gravity) (rib cage and ligaments not shown for clarity). (H) Simulated gravity, supine on the bed (rib cage and ligaments not shown for clarity). (I) Supine in-brace (green) patient (rib cage and ligaments not shown for clarity).

the external soft tissues by quadrilateral shell elements. Mechanical properties were taken from experimental and published data [16,17,22,30].

The center of gravity of the trunk slices corresponding to each vertebra was derived from the literature [31-34] and scaled according to patient's size and assumed to follow the scoliotic curve in the coronal plane. The magnitude of the gravitational forces associated with each slide was scaled to the patient's specific weight based on published values [31,34].

The interior surface of each patient's brace was digitized using a laser beam scanner (FastSCAN, Polhemus, Colchester, VT, USA). The acquired geometry was post-processed using a CAD/CAM software (Rodin4D, Bordeaux, France) and the FEM of the brace was then generated. The brace external polyethylene shell was modeled by four-node quadrilateral shell elements with linear elastic properties (E = 1500 MPa, ν = 0.3) [16,35]. A surface-to-surface contact interface taking friction into account (friction coefficient of 0.6) [36] was created between the brace and trunk models.

Supine position simulation

Because the radiographs were acquired in the standing position, a simulation was necessary to compute the transition from standing to supine position. The technique was described in detail in previous works [21,37] and is here summarized.

The global forces and moments acting on the vertebral endplates and the axial compressive stresses in the spine were in a local coordinate system for each vertebra (z-axis in the upward direction [axial], x-axis in the anterior direction, and y-axis to the left of the patient; Fig. 1F). Upward-directed vertical forces were applied to find the zero-gravity geometry. During this step, the pelvis was fixed in space, and the translation of the first thoracic vertebra was blocked in the transverse plane. The bed surface was modeled parallel to the coronal plane, and contact interfaces with frictional forces were created between the trunk and bed models (Fig. 1G–I). Posteriorly directed forces representing gravitational forces were applied to the corresponding centers of gravity's nodes to

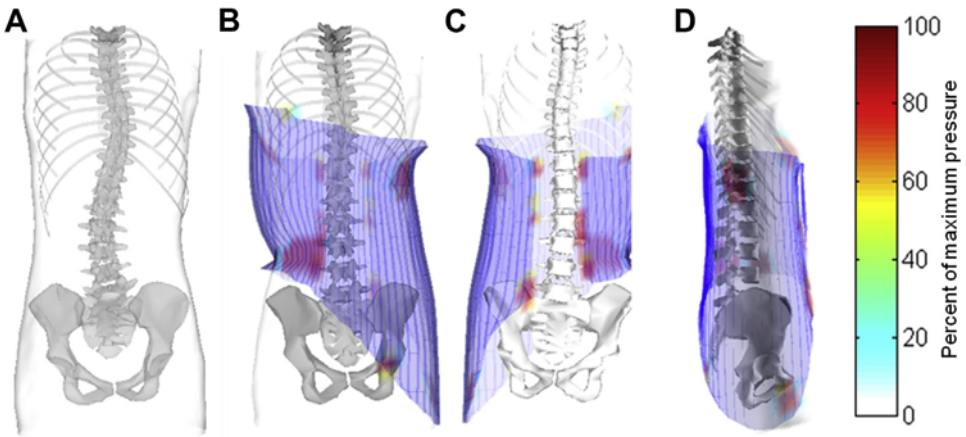

Fig. 2. Simulation of the brace worn by the patient (bed not shown). (A) Posterior view of standing FEM without brace. (B, C, D) Posterior, anterior and lateral views of supine FEM in brace. The color code represents the relative pressure with respect to the maximum pressure.

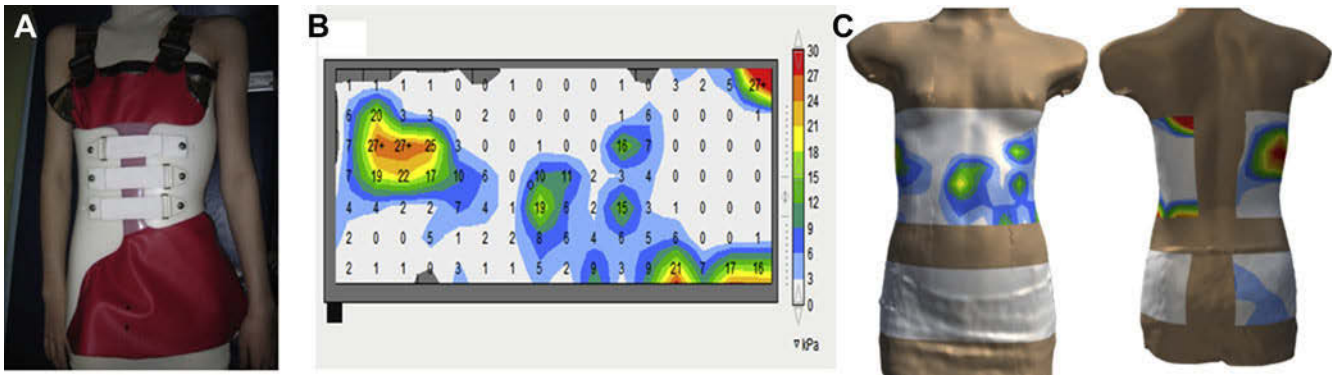

Fig. 3. Brace pressure measurement. (A) Pressure mat (in red) wrapped around the patient's torso under the brace. (B) Graphical representation of measured pressures using FSA 4.1 software (VERG, Winnipeg, Canada) (unwrapped pressure mat). (C) Graphical visualization (reconstruction) of patient's torso with pressure mat in place (anterior and posterior views).

find the geometry of the patient in the supine position (Fig. 1H). During this step, the pelvis was free to rotate around the y-axis. The only boundary condition applied was the blocked translations of T1 and S1 along the y-axis. It was the contact interface with the bed model that constrained the trunk along the x-axis.

Simulation of the brace installation

The brace installation on the patient was simulated in 2 steps. The brace was first opened by applying displacements on four nodes located in its anterior part and was positioned on the patient. Then, two or three sets of collinear forces of 60 N representing the existing thoracic, lumbar, and pelvic straps were applied on the nodes corresponding to the strap fixations on the anterior part of the brace [38].

During the whole process, the contact interface between the trunk and the brace models as well as the contact interface between the brace and the bed models constrained the entire model in the posteroanterior x-axis direction. In addition, the pelvis translation was blocked in the y- and z-axis directions whereas T1 was free to move along the y- and z-axis directions.

Once the simulation was completed, several indices were computed: Cobb angles, kyphosis and lordosis, apical vertebral axial rotation, bending moments at each vertebral level, and the pressures generated by the brace on the patient's trunk (Fig. 2).

Cutaneous pressure measurements

For the last 11 recruited patients, pressures at the interface between the Providence brace and the skin were measured for verification purposes using a pressure mapping system consisting of a dual-pressure mattress of 16 × 7 and 16 × 5 sensors (Vista Medical, Winnipeg, Canada). The sensors have a registration limit of 26.7 kPa (200 mmHg) and an accuracy of ± 5 mmHg (0.7 kPa). The pressures were registered during 30 seconds, and the average pressure distribution was computed for each zone corresponding to the corrective bolsters on the measurement board (Fig. 3).

Results

Eighteen patients with AIS were consecutively recruited from our outpatient clinic after a Providence brace was prescribed by the treating orthopedic surgeon, between September 2012 and March 2013, with the approval of our hospital ethical committee (Table 1). Among the patients, there were 16 girls and 2 boys. Eight patients had single thoracolumbar/lumbar curves (P1–P8), one patient had a single thoracic curve (P9), and nine patients had double curves (P10–P18). The average Cobb angle was 26.1 degrees (12–40 degrees) and 28.8 degrees (14–42 degrees) for thoracic and lumbar curves, respectively. Mean curve correction in Providence brace as measured on supine in-brace X-ray was 65% and 70% of the initial thoracic and lumbar curves, respectively. Average chronological age of the patients was 12.8 years (10-16 years). Four patients had Risser 0, four had Risser 1, three had Risser 2, two had Risser 3, and five had Risser 4.

Curve correction simulation

The simulated average curve correction induced by the transition from standing to supine position was 45% and 48% for thoracic and lumbar curves, respectively. After the simulation of brace installation, average correction was 60% for thoracic curves and 64% for thoracolumbar/lumbar curves. The mean absolute difference between the simulated and real in-brace Cobb angles was 3.4 and 4.6 degrees for thoracic and lumbar curves, respectively. The difference for each case could be seen in Table 1. The 95% confidence interval (CI) for thoracic Cobb angles is ±4.5 degrees for the Providence brace, ±3.0 degrees for simulated supine, and ±3.6 degrees for the simulated brace. Further, the 95% CI for thoracolumbar/lumbar Cobb angles is ±4.1 degrees for the Providence brace, ±1.9 degrees for simulated supine; and ±3.3 degrees for the simulated brace.

Table 1
Demographic data and Cobb angle comparison between out of brace initial-standing (Stand), supine Providence-in-brace (Pro), simulated–supine out of brace (Sim Supine), and simulated in-brace supine (Sim Brace) for each case.

Case	Age (years)	Risser	Thoracic Cobb Angle[a,b] (Degrees)					Lumbar Cobb Angle[a] (Degrees)				
			Stand	Pro	Sim Supine	Sim Brace	Absolute Difference (Pro–Sim Brace)	Stand	Pro	Sim Supine	Sim Brace	Absolute Difference (Pro–Sim Brace)
P01	15	4	–	–	–	–		20	1	14	11	10
P02	14	1	–	–	–	–		24	−9	8	−5	4
P03	11	0	–	–	–	–		23	10	15	15	5
P04	10	0	–	–	–	–		29	7	15	5	2
P05	12	1	12	1	5	3	2	28	9	15	12	3
P06	13	0	13	6	8	6	0	28	6	15	10	4
P07	12	0	14	−15	6	−7	8	20	−12	11	−8	4
P08	14	4	19	7	10	10	3	29	6	16	12	6
P09	13	2	25	8	16	14	6	14	7	5	8	1
P10	14	4	35	10	20	16	6	37	11	17	14	3
P11	12	3	26	10	13	8	2	33	22	18	16	6
P12	14	2	26	16	17	13	3	35	19	20	23	4
P13	13	3	34	13	15	9	4	29	6	16	13	7
P14	11	2	23	8	9	7	1	30	21	12	9	12
P15	16	4	40	23	23	19	4	33	17	16	14	3
P16	12	1	30	17	18	17	0	26	13	15	12	1
P17	14	4	38	16	23	18	2	42	14	23	12	2
P18	11	1	30	9	17	15	6	38	10	20	16	6
Mean	12.8	2.0	26.1	7.5	11.4	8.3	3.4	28.8	8.8	15.1	10.5	4.6
SD	1.5	1.5	8.8	8.6	5.7	6.8	2.3	6.8	8.8	4.1	7.1	2.8
95% CI			4.6	4.5	3.0	3.6	1.2	3.2	4.1	1.9	3.3	1.3

SD, standard deviation; CI, confidence interval.
[a] Negative sign means inversion of curve to the opposite side.
[b] Thoracic Cobb angle <10 degrees are not registered.

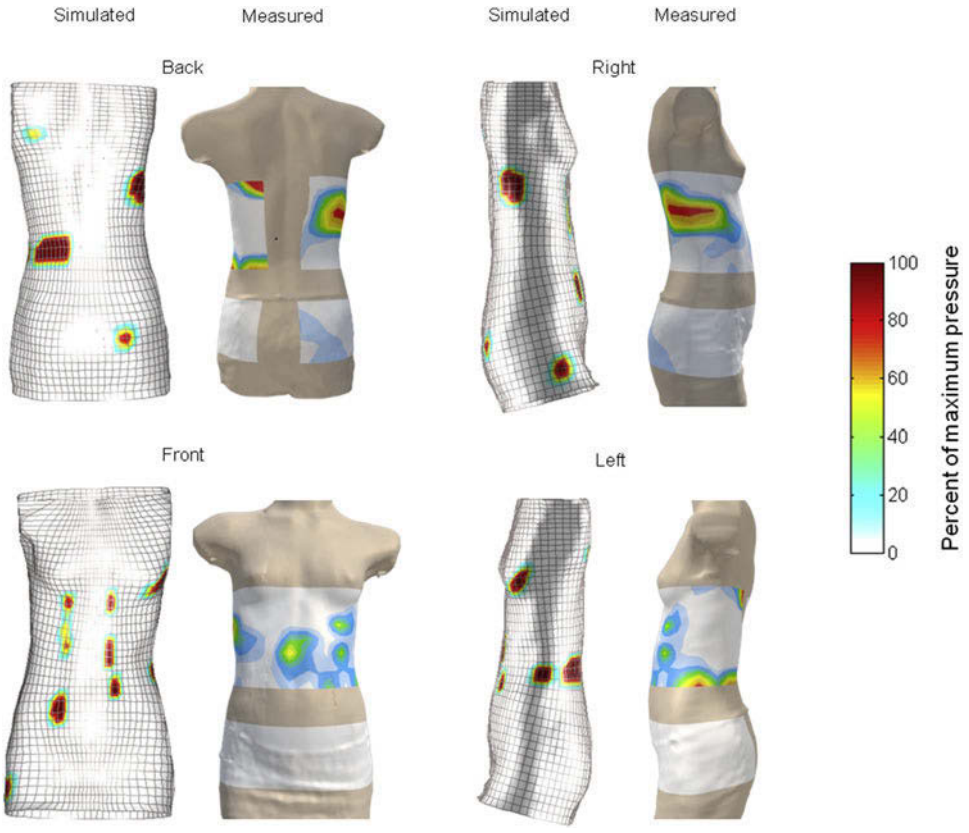

Fig. 4. Simulated pressures compared to the measured pressures for patient P16.

Table 2
Simulated moments (in N•mm) in the coronal plane generated at the apex of the curves in the initial standing position (Sim Stand), in the simulated supine position (Sim Supine), and with the simulated Providence brace (Sim Brace) for thoracic and lumbar curves.

Case	Thoracic Curve				Lumbar Curve			
	Apex	Sim Stand	Sim Supine (% Reduction)	Sim Brace (% Reduction)	Apex	Sim Stand	Sim Supine (% Reduction)	Sim Brace (% Reduction)
P01	–	–	–	–	T12	−259	−6 (98%)	60 (123%)
P02	–	–	–	–	L3	−589	−0.1 (100%)	81 (114%)
P03	–	–	–	–	T12	−366	0 (100%)	23 (106%)
P04	–	–	–	–	L2	−1243	−0.4 (100%)	87 (107%)
P05	T7	60	0 (100%)	−12 (120%)	T12	−379	−2 (99%)	41 (111%)
P06	T8	100	−0.5 (101%)	−15 (115%)	L2	−353	−3.9 (99%)	54 (115%)
P07	T8	89	−0.8 (101%)	−6 (107%)	T12	−301	1.8 (101%)	38 (113%)
P08	T6	121	−3.7 (103%)	1 (99%)	T12	−474	1.8 (100%)	31 (107%)
P09	–	–	–	–	T11	250	0.7 (100%)	−37 (115%)
P10	T10	305	−1.9 (101%)	−30 (110%)	L3	−800	11.4 (101%)	41 (105%)
P11	T8	103	−1.2 (101%)	−22 (121%)	L3	−334	−2.1 (99%)	34 (110%)
P12	T6	56	1.4 (98%)	−13 (123%)	L3	−256	2.3 (101%)	39 (115%)
P13	T8	146	−1.8 (101%)	−25 (117%)	L1	−459	−2.2 (100%)	83 (118%)
P14	T9	280	−0.9 (100%)	−58 (121%)	L2	−405	0.1 (100%)	−40 (90%)
P15	T10	367	−3.8 (101%)	−50 (114%)	L3	−542	0.2 (100%)	84 (115%)
P16	T8	247	−2.3 (101%)	−13 (105%)	L3	−410	0.3 (100%)	54 (113%)
P17	T8	343	−0.3 (100%)	−37 (111%)	L3	−1263	−2.4 (100%)	69 (105%)
P18	T8	231	−0.6 (100%)	−25 (111%)	L3	−881	1.6 (100%)	36 (104%)
Average		193	−1.3 (101%)	−23 (113%)		−504	0.1 (100%)	43 (110%)

%Reduction is the ratio of simulated correction of the bending moment with respect to that in the simulated standing posture (percentage above 100% indicates an overcorrection in the opposite direction).

Simulated correction of apical vertebral rotation was inconsistent between cases, with an overall average correction of less than 2 degrees. From average initial apical vertebral rotation of 6 and 8 degrees for thoracic and lumbar curves respectively, the simulated supine position reduced them to an average of 5 and 7 degrees, respectively, whereas the simulations of Providence brace had little effect on average thoracic and lumbar apical vertebral rotation (5 and 8 degrees, respectively). Simulated transition from standing to supine position reduced kyphosis and lordosis by an average of 42%, whereas simulated brace application resulted in a total average reduction of kyphosis and lordosis by 75%.

Model verification using torso pressures

Measurement of pressures revealed two major pressure zones: thoracic (lateral) and opposing lumbar (posterolateral). These pressure zones corresponded to skin areas pressured by the corrective bolsters. Simulated brace pressures were in the same regions as experimentally measured pressures (Fig. 4).

Bending moments exerted on vertebrae

Simulated gravity in standing position induced bending moments on vertebrae (average 199 N•mm at the thoracic apical level, and 504 N•mm at the lumbar apical level), representing asymmetrical compressive loading of vertebral endplates (Table 2; Sim Stand columns). They were mostly annulled by the positioning in the supine position (Table 2; Sim Supine columns), and further overcorrected on average by 10% to 13% (maximum 23%) (Table 2; Sim Brace columns), but in the opposite direction.

Discussion

This is the first computational biomechanical study of the Providence nighttime brace. The FEM incorporates gravitational forces and a supine position opposing to a horizontal surface, which allows a better understanding of corrective mechanisms of the Providence brace for nighttime treatment of adolescent idiopathic scoliosis. The supine position changes the orientation of the gravity forces acting along the spine longitudinal axis, and the interaction with the horizontal surface of the bed induces a correction of the scoliotic curves. Mean simulated correction (48%) is slightly greater than the reported 37% mean reduction in larger curves attributed to the intraoperative prone position (patient lying on four-post positioning table) as reported by Delorme [12]. The simulated brace resulted in 15% additional correction on average. Therefore, the supine position was responsible for the major part of the total correction (average = 63%).

When considering all cases, brace correction was inferior to reported values [7,9-11]. When subdividing cases based on curve type (single vs. double curves), the curve correction of the single curve subgroup was significantly greater (88% vs. 56%). Also, patients with thoracolumbar/lumbar curves >20 degrees and main thoracic curves <20 degrees (P1–P8) had the best correction (94% in Providence brace, 45% supine, and 75% in simulated brace).

Brace application reduced significantly kyphosis and lordosis, while having only a minor effect on apical vertebral rotation. This suggests that curve correction was principally in the coronal plane without a significant correction in the transverse plane, with limited three-dimensional correction.

The measured and simulated in-brace skin pressure distribution followed the expected lateral three-point pressure pattern, a two-dimensional principle that is also documented in the orthotic literature [36,39-41]. Additional pressures on the back, coming from the gravity exerted on supine patient trunk and its interaction with the bed support, represent an additional correction mechanism that reduced the sagittal and coronal curvatures. The pressure mapping system, however, had a registration limit of 26.7 kPa, and measured pressures often exceeded this value, which saturated the sensors and restrained the possibility of full comparison and validation between measured and simulated pressures. The saturated high-pressure areas ($>$26.7 kPa) were analogous to pressure areas reported by brace developers in their published work (37.9 and 51 kPa for thoracic and lumbar zones, respectively) [7], but higher than experimental measures reported by Mac-Thiong (between 10 and 30 kPa) with daytime brace in the standing posture [38].

The reduction of the resulting coronal plane bending moments exerted on the vertebrae revealed another corrective mechanism allowing reducing the asymmetrical compressive loading of the vertebral epiphyseal growth plates in the coronal plane. Initially, the compressive loads as a result of the offset of the gravity on the spinal curvature were greater on the concave side of the curves; they were then mostly annulled in the supine position, and shifted to the convex side after brace application. This reduction and further inversion of asymmetrical loading pressures on the vertebral endplates would favor the reduction of asymmetric growth of the spine and its correction according to the Hueter-Volkmann principle [42-44]. However, more investigation of pressures exerted on epiphyseal vertebral growth plates is necessary to better assess such correction mechanism.

Only immediate supine and in-brace corrections were simulated, and long-term outcome of the treatment could only be deduced by analyzing the asymmetrical pattern of the compressive stresses acting on the growth plates. However, correlations between immediate in-brace correction and long-term effect of bracing have been reported [45,46]. In the future, models allowing explicit representation of the growth modulation process [21] could be included in the simulation process in order to analyze the long-term effect of the brace.

The model has some limitations, such as not including muscular activity. This would probably have a marginal impact on the conclusions since the patient would be asleep during brace wear. The intervertebral discs and vertebrae were represented by beam elements without taking into account the hydrostatic behavior of the nucleus, which might affect the load distribution on the growth plates. Also, the inclusion of Risser 3 and 4 cases in our study may have limited the comparability of our results with clinical results of Providence brace reported in the literature, because these patients are generally excluded from clinical studies as they do not fit the criteria of the Scoliosis Research Society (SRS). The exclusion of the seven cases with Risser 3 and 4 would have increased the average in-brace correction to 72% for thoracic curves and 73% for lumbar curves, which is closer to published results.

With such models, an interesting perspective could be to leverage its capability to include various brace design configurations (such as brace shape, material, thickness, strap position and tension, etc) to further analyze their effects and optimize the brace effectiveness before its fabrication and delivery to the patients.

Conclusions

The computational finite element model used in this study allowed to simulate and analyze individually the biomechanics of supine posture and the application of nighttime Providence brace. The supine position is responsible for the major part of the coronal plane curve correction, whereas the Providence brace itself plays a complementary role in curve correction by inverting the bending moments acting on vertebral growth plates. It confirmed the two-dimensional three-point pressure action principle of the brace assumed by its designers. Bending moments induced by the brace generated a rebalancing of pressure on the growth plates, which could reduce the asymmetric growth of the vertebrae according to Hueter-Volkmann principle.

Acknowledgments

Project supported by the NSERC (Natural Sciences and Engineering Research Council of Canada, Grant number RGPIN239148-11) and the CIHR (Canadian Institutes of Health Research, Grant number 259812). Special thanks to Frédérique Desbiens-Blais, Isabelle Turgeon, Benoit Bissonnette, Marie-Chantal Bolduc, Manivone Savann, Dr. Stefan Parent, and Dr. Benoit Poitras for their participation in this study.

References

[1] Weinstein SL, Dolan LA, Wright JG, Dobbs MB. Effects of bracing in adolescents with idiopathic scoliosis. *N Engl J Med* 2013;369:1512–21.

[2] Brox J, Lange J, Gunderson R, Steen H. Good brace compliance reduced curve progression and surgical rates in patients with idiopathic scoliosis. *Eur Spine J* 2012;21:1957–63.

[3] Rahman T, Bowen JR, Takemitsu M, Scott C. The association between brace compliance and outcome for patients with idiopathic scoliosis. *J Pediatr Orthop* 2005;25:420–2.

[4] Katz DE, Herring JA, Browne RH, et al. Brace wear control of curve progression in adolescent idiopathic scoliosis. *J Bone Joint Surg* 2010;92:1343–52.
[5] Climent JM, Sanchez J. Impact of the type of brace on the quality of life of adolescents with spine deformities. *Spine (Phila Pa 1976)* 1999;24:1903–8.
[6] Price CT, Scott DS, Reed Jr FR, et al. Nighttime bracing for adolescent idiopathic scoliosis with the Charleston Bending Brace: long-term follow-up. *J Pediatr Orthop* 1997;17:703–7.
[7] d'Amato CR. Griggs S, McCoy B. Nighttime bracing with the providence brace in adolescent girls with idiopathic scoliosis. *Spine* 2001;26:2006–12.
[8] d'Amato CR, McCoy B. *The Providence Scoliosis System*. Milwaukee, WI: Scoliosis Research Society; 2003.
[9] Yrjonen T, Ylikoski M, Schlenzka D, et al. Effectiveness of the Providence nighttime bracing in adolescent idiopathic scoliosis: a comparative study of 36 female patients. *Eur Spine J* 2006;15:1139–43.
[10] Janicki JA, Poe-Kochert C, Armstrong DG, et al. A comparison of the thoracolumbosacral orthoses and providence orthosis in the treatment of adolescent idiopathic scoliosis: results using the new SRS inclusion and assessment criteria for bracing studies. *J Pediatr Orthop* 2007;27:369–74.
[11] Bohl DD, Telles CJ, Golinvaux NS, et al. Effectiveness of providence nighttime bracing in patients with adolescent idiopathic scoliosis. *Orthopedics* 2014;37:e1085–90.
[12] Delorme S, Labelle K, Poitras B, et al. Pre-, intra-, and postoperative three-dimensional evaluation of adolescent idiopathic scoliosis. *J Spinal Disord* 2000;13:93–101.
[13] Duke K, Aubin CE, Dansereau J, Labelle H. Biomechanical simulations of scoliotic spine correction due to prone position and anaesthesia prior to surgical instrumentation. *Clin Biomech* 2005;20:923–31.
[14] Wynarsky GT, Schultz AB. Optimization of skeletal configuration: Studies of scoliosis correction biomechanics. *J Biomech* 1991;24:721–32.
[15] Gignac D, Aubin CE, Dansereau J, Labelle H. Optimization method for 3D bracing correction of scoliosis using a finite element model. *Eur Spine J* 2000;9:185–90.
[16] Perie D, Aubin CE, Lacroix M, et al. Biomechanical modelling of orthotic treatment of the scoliotic spine including a detailed representation of the brace-torso interface. *Med Biol Eng Comput* 2004;42:339–44.
[17] Périé D, Aubin CE, Petit Y, et al. Personalized biomechanical simulations of orthotic treatment in idiopathic scoliosis. *Clin Biomech* 2004;19:190–5.
[18] Clin J, Aubin CE, Labelle H. Virtual prototyping of a brace design for the correction of scoliotic deformities. *Med Biol Eng Comput* 2007;45:467–73.
[19] Desbiens-Blais F, Clin J, Parent S, et al. New brace design combining CAD/CAM and biomechanical simulation for the treatment of adolescent idiopathic scoliosis. *Clin Biomech* 2012;27:999–1005.
[20] Cobetto N, Aubin CE, Clin J, et al. Braces optimized with computer-assisted design and simulations are lighter, more comfortable, and more efficient than plaster-cast braces for the treatment of adolescent idiopathic scoliosis. *Spine Deform* 2014;2:276–84.
[21] Clin J, Aubin CE, Parent S, Labelle H. A biomechanical study of the Charleston brace for the treatment of scoliosis. *Spine* 2010;35:E940–7.
[22] Clin J, Aubin CE, Parent S, et al. Comparison of the biomechanical 3D efficiency of different brace designs for the treatment of scoliosis using a finite element model. *Eur Spine J* 2010;19:1169–78.
[23] Desbiens-Blais F, Clin J, Parent S, et al. CAD/CAM and biomechanical simulations vs. standard technique for the design of braces in adolescent idiopathic scoliosis: first results. *Scoliosis* 2013;8. O41.
[24] Driscoll CR, Aubin CE, Canet F, et al. Impact of prone surgical positioning on the scoliotic spine. *J Spinal Disord Tech* 2012;25:173–81.
[25] Cobetto N, Aubin CE, Parent S, et al. Effectiveness of braces designed using computer aided design and manufacturing (CAD/CAM) and finite element simulation compared to CAD/CAM only for the conservative treatment of adolescent idiopathic scoliosis: a prospective randomized controlled trial. *Eur Spine J* 2016.
[26] Bertrand S, Laporte S, Parent S, et al. Three-dimensional reconstruction of the rib cage from biplanar radiography. *IRBM* 2008;29:278–86.
[27] Humbert L, de Guise JA, Aubert B, et al. 3D reconstruction of the spine from biplanar X-rays using parametric models based on transversal and longitudinal inferences. *Med Eng Phys* 2009;31:681–7.
[28] Pazos V, Cheriet F, Danserau J, et al. Reliability of trunk shape measurements based on 3-D surface reconstructions. *Eur Spine J* 2007;16:1882–91.
[29] Fortin D, Cheriet F, Beauséjour M, et al. 3D visualization tool for the design and customization of spinal braces. *Comput Med Imaging Graph* 2007;31:614–24.
[30] Aubin CE, Dansereau J, de Guise JA, Labelle H. A study of biomechanical coupling between spine and rib cage in the treatment by orthosis of scoliosis [in French]. *Ann Chir* 1996;50:641–50.
[31] Cheng CK, Chen HH, Chen CS, et al. Segment inertial properties of Chinese adults determined from magnetic resonance imaging. *Clin Biomech (Bristol, Avon)* 2000;15:559–66.
[32] Liu YK, Laborde JM, Van Buskirk WC. Inertial properties of a segmented cadaver trunk: their implications in acceleration injuries. *Aerosp Med* 1971;42:650–7.
[33] Pearsall DJ, Reid JG, Livingston LA. Segmental inertial parameters of the human trunk as determined from computed tomography. *Ann Biomed Eng* 1996;24:198–210.
[34] Pearsall DJ, Reid JG, Ross R. Inertial properties of the human trunk of males determined from magnetic resonance imaging. *Ann Biomed Eng* 1994;22:692–706.
[35] Sanders JE, Greve JM, Mitchell SB, Zachariah SG. Material properties of commonly-used interface materials and their static coefficients of friction with skin and socks. *J Rehabil Res Dev* 1998;35:161–76.
[36] Emans J. *The Bracing Manual, The Boston Brace*. Milwaukee, WI: Scoliosis Research Society; 2003.
[37] Clin J, Aubin CE, Lalonde N, et al. A new method to include the gravitational forces in a finite element model of the scoliotic spine. *Med Biol Eng Comput* 2011;49:967–77.
[38] Mac-Thiong JM, Petit Y, Aubin CE, et al. Biomechanical evaluation of the Boston brace system for the treatment of adolescent idiopathic scoliosis: relationship between strap tension and brace interface forces. *Spine* 2004;29:26–32.
[39] Fayssoux RS, Cho RH, Herman MJ. A history of bracing for idiopathic scoliosis in North America. *Clin Orthop Relat Res* 2010;468:654–64.
[40] Galante J, Schultz A, Dewald RL, Ray RD. Forces acting in the Milwaukee brace on patients undergoing treatment for idiopathic scoliosis. *J Bone Joint Surg* 1970;52:498–506.
[41] Lonstein J. *The Bracing Manual, The Milwaukee Brace*. Milwaukee, WI: Scoliosis Research Society; 2003.
[42] Roaf R. Vertebral growth and its mechanical control. *J Bone Joint Surg* 1960;42-B:40–59.
[43] Stokes IA, Bigalow LC, Moreland MS. Measurement of axial rotation of vertebrae in scoliosis. *Spine (Phila Pa 1976)* 1986;11:213–8.
[44] Castro Jr FP. Adolescent idiopathic scoliosis, bracing, and the Hueter-Volkmann principle. *Spine J* 2003;3:180–5.
[45] Emans JB, Kaelin A, Bancel P, et al. The Boston bracing system for idiopathic scoliosis. Follow-up results in 295 patients. *Spine (Phila Pa 1976)* 1986;11:792–801.
[46] Katz DE, Durrani AA. Factors that influence outcome in bracing large curves in patients with adolescent idiopathic scoliosis. *Spine (Phila Pa 1976)* 2001;26:2354–61.